UNIVERSITY OF Southampton

Modeling and Control Optimization of an Engine

24-25 Ships Engine automation and testing

Tianhang Zhao

26/6/2025

Abstract

This project focuses on modeling, analysis, and control of a heavy-duty diesel engine based on the Cummins N14. An ideal Otto cycle model was developed in MATLAB/Simulink and parameterized using reference data. Key parameters such as fuel injection timing, quantity, intake pressure, and air-fuel ratio were varied to analyze their impact on engine performance metrics including torque, power, thermal efficiency, and BSFC. A closed-loop PID control system with a 2-D Lookup Table was implemented to track target torque under dynamic conditions. Control strategy optimization was explored to improve performance in terms of accuracy.

Introduction

The performance of modern engines is increasingly governed by advanced electronic control strategies, particularly through the Engine Control Unit (ECU), which directly influences power output, fuel consumption, and emission levels. To support the development of such strategies, this project presents a comprehensive modeling and control study based on the Cummins N14 heavy-duty diesel engine. A thermodynamic model grounded in the ideal Otto cycle is constructed and calibrated using real engine parameters. The model is then used to perform a systematic sensitivity analysis of key input variables—such as fuel injection quantity, injection timing, intake pressure, and air-fuel ratio — on output torque, power, thermal efficiency, and brake-specific fuel consumption (BSFC). Based on these insights, a closed-loop control system combining PID feedback and feedforward lookup tables is implemented to track target torque profiles under dynamic conditions. Finally, advanced control strategies, such as gain scheduling, are explored to further improve performance, laying the groundwork for efficient, real-time engine management.

Tasks

I. Modify Model Parameters and Implement Combustion Completeness Based on Equivalence Ratio

The diesel engine model selected and simulated in this study is the classic Cummins N14 series engine, which is a turbocharged, intercooled, direct-injection diesel engine with an inline six-cylinder, four-stroke configuration. The fundamental specifications of the engine are summarized in Table 1.

Table.1 Cummins N14 production engine

Cylinder bore X stroke (mm)	140 X 152
Connecting rod length (mm)	305.
Displacement volume (L)	2.34
Compression ratio	10:1
Inlet air pressure	166 kPa
Inlet air temperature	423 K

Swirl ratio (nominal)	1.0
Engine speed	600~1800 rpm
Fuel	blended (68% heptamethylnonane and 32% hexadecane)
Injection pressure	84 MPa (peak)
Fuel injected	0.0553 g/cycle
Start of injection	-10. 0 deg. ATDC
Inlet pressure range	100～280kPa
Rated power	300kW

Subsequently, a basic Simulink model of the Otto cycle was constructed, as illustrated in Figure 1. In this model, it is assumed that the fuel undergoes instantaneous combustion, frictional losses are neglected, and both the in-cylinder pressure and temperature are reset at the end of each cycle. Additionally, a logical conditional statement was incorporated to evaluate whether the fuel can be completely combusted, in accordance with the specified requirements.

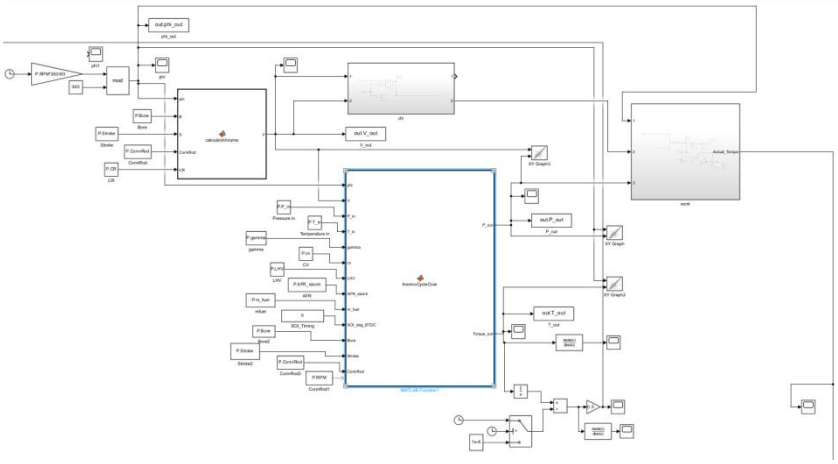

Fig.1. Otto cycle model in simulink

II. Compare Model Outputs with Reference Engine Data and Analyze Discrepancies

The key reason for the discrepancy lies in the idealized nature of the Otto cycle model compared to the real Cummins N14 diesel engine. The model assumes instantaneous and complete combustion, no heat transfer, no friction, and no pumping losses—conditions that do not hold in reality. As a result, the simulated thermal efficiency reaches 58.8%,

much higher than the reference value of 41.3%. Consequently, the model's BSFC is only 144 g/kWh, compared to 212 g/kWh in the real engine. These differences are mainly due to the absence of heat losses, mechanical friction, and incomplete combustion in the model. Similarly, the model predicts a peak torque of 2500 N·m and average power of 20.7 kW, which exceed typical real engine values, as the model assumes all indicated work is fully converted to output without internal losses.

Table.2 Cummins N14 production engine

	Thermal Efficiency (%)	BSFC (g/kWh)	Peak Torque (N·m)	Power (kW)
Model Outputs	58.8	144	2500	20.7
Reference	41.3	212	1500	14.1

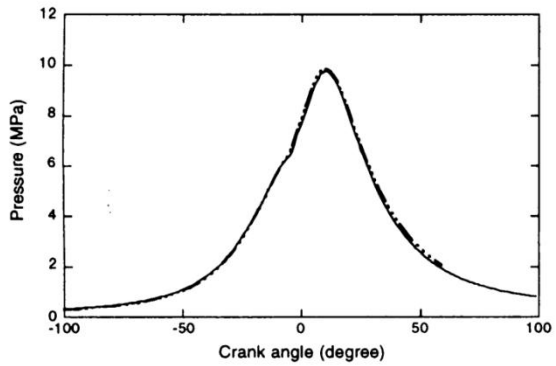

Fig.2 Reference Cylinder pressure curve

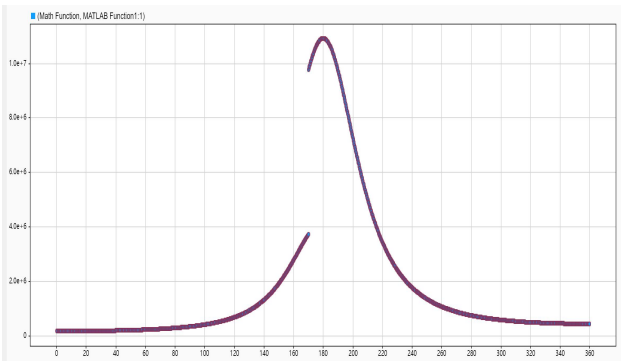

Fig.3 Model Output Cylinder pressure curve

III. Analyze Effects of Injection Timing, Fuel Quantity, Intake Conditions, and Air-Fuel Ratio on Engine Performance and Cylinder Pressure/Temperature/Volume Diagrams

This study is based on a series of Simulink simulation results and aims to analyze the effects of various input parameters on the performance of an ideal Otto cycle model of the Cummins N14 engine. The parameters investigated include intake pressure, fuel injection quantity, injection timing, and air–fuel ratio. The results are as fellow.

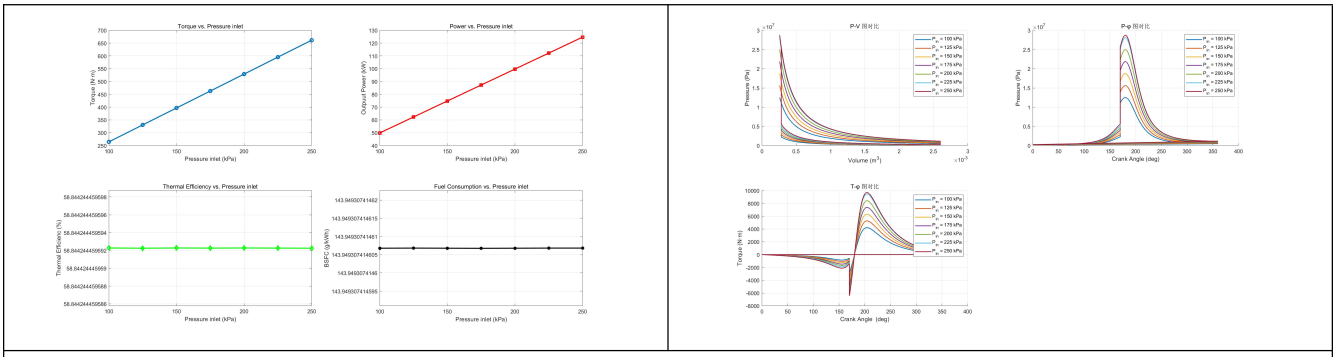

Fig.4 Different Pressure inlet

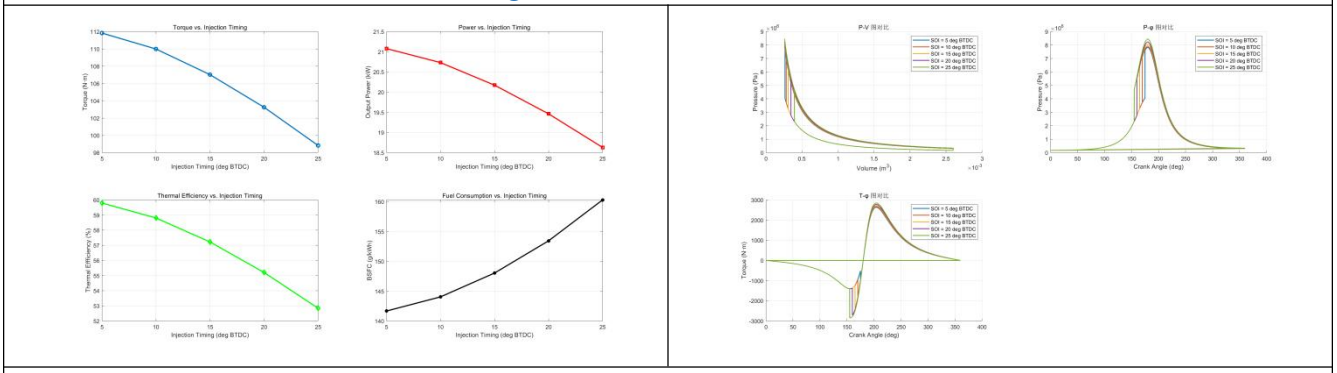

Fig.5 Different Injection timing

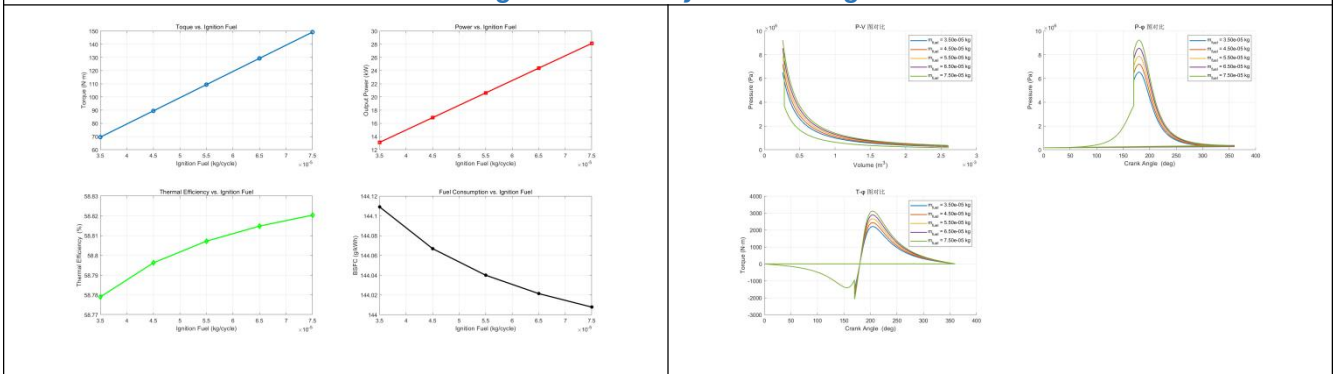

Fig.6 Different Fuel injection quantity

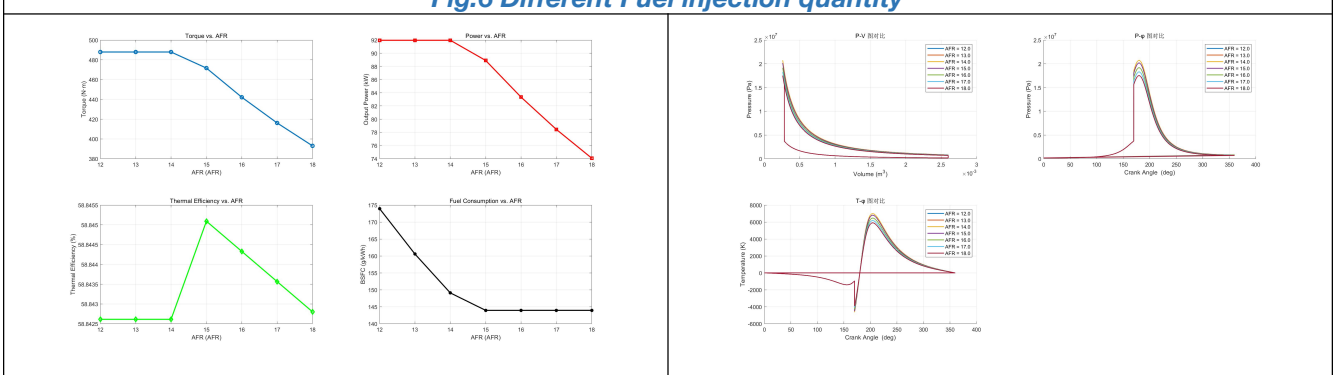

Fig.7 Different AFR

Inlet Pressure： At rated engine speed, when the intake pressure $\mathrm{P_{in}}$ increases while the fuel injection mass $\mathrm{m_{fuel}}$ remains constant, the simulation results show a linear decrease in torque, thermal efficiency, and power output. This trend is attributed to the significant rise

in the air-fuel ratio (AFR), which leads to an excessively lean mixture and reduced combustion efficiency.

A lean mixture causes ignition difficulties and slows flame propagation, thereby delaying the combustion process. As a result, peak cylinder pressure occurs after the piston has already started descending, reducing the effectiveness of the expansion stroke. Additionally, the slower heat release increases heat losses through the cylinder walls, further lowering thermal efficiency. Consequently, the indicated mean effective pressure (IMEP) drops sharply, and both torque and power output decrease significantly, indicating poor energy utilization.

This phenomenon appears counterintuitive in practical engineering contexts, where increased intake pressure is generally expected to enhance charge efficiency and power output. Therefore, to better assess the effect of intake pressure, the fuel injection mass was proportionally increased in subsequent simulations to maintain an approximately constant AFR.

Fuel Injection Mass：When the fuel injection mass was increased from 3.5 to 7.5 e-5kg/cycle, the torque rose from 70 N·m to 150 N·m, and power increased from 13 kW to 28 kW. The thermal efficiency slightly improved (from 58.78% to 58.82%), and the brake-specific fuel consumption (BSFC) decreased (from 144.1 to 144.0 g/kWh). The P–ϕ diagram showed a significant rise in peak pressure with increased fuel, while the area enclosed by the P–V diagram expanded, indicating higher cycle work output.

Start of Injection：When the injection timing was advanced from 5° BTDC to 25° BTDC, torque decreased from 112 N·m to 98 N·m, and BSFC increased from 142 g/kWh to 160 g/kWh. Excessively early injection led to combustion occurring during the compression stroke, generating negative work that offset part of the expansion work, thus reducing overall efficiency. The P–ϕ diagram showed that the pressure peak appeared earlier, and the loop area in the P–V diagram shrank, confirming a drop in net work output.

Air-Fuel Ratio (AFR)：When AFR increased from 12 to 14.5, torque and power remained high (approximately 485 N·m and 92 kW), with thermal efficiency peaking around AFR = 14.5 (58.845%) and the lowest BSFC (approximately 143.9 g/kWh). However, when AFR

exceeded 14.5, the reduced fuel amount led to lower heat release, resulting in decreased pressure and temperature peaks, which in turn caused both performance and efficiency to decline.

IV. *Solve the optimal parameters of fuel-air relationship and thermal efficiency under multiple operating conditions*

1 Injection time for optimal thermal efficiency

From the simulation results in Question 3, it can be observed that, under the ideal Otto cycle model, increasing the fuel injection (or ignition) advance angle leads to a significant decrease in thermal efficiency. Although this result is mathematically valid within the idealized model, it contradicts the operating characteristics of real engines. In practice, as engine speed increases, a larger injection advance angle is typically required—a phenomenon rooted in the temporal characteristics of the combustion process.

In real internal combustion engines, fuel ignition and combustion are chemical processes that unfold over a finite period of time, typically lasting several milliseconds (ms), largely independent of changes in crankshaft speed. In contrast, piston motion is linearly related to engine speed, so the duration of each stroke decreases as RPM increases. For example, when engine speed rises from 1000 rpm to 2000 rpm, the time required to complete one stroke is reduced from approximately 30 ms to 15 ms. Under high-speed conditions, the same combustion duration spans a significantly greater crank angle. Therefore, to ensure that combustion completes slightly after the piston reaches Top Dead Center (TDC)—the point at which mechanical work output is maximized—the fuel injection timing must be advanced accordingly. This ensures sufficient time for fuel mixing, ignition, and combustion.

In other words, in real engines, increasing the injection (or ignition) advance angle is not intended to complete combustion earlier, but rather to ensure that it finishes at the "optimal timing"—specifically, when the pressure peak acts on the piston just after it starts its downward motion. If ignition is too late, the piston has already moved far from TDC, the cylinder volume increases, pressure drops, and energy conversion efficiency diminishes. If ignition is too early, the combustion pressure significantly resists the piston's upward

motion, generating negative work and potentially damaging mechanical components (as illustrated in Figure 10,11).

However, the ideal Otto cycle model—as used in this simulation study—assumes "instantaneous combustion," meaning that all heat is released at a single specified crank angle. This assumption ignores the time required for combustion and thus fails to capture the beneficial effects of advancing the injection angle. Instead, the earlier the heat is added, the more likely it is to generate a counteracting force on the piston during the compression stroke, resulting in reduced thermal efficiency.

Therefore, the combustion model was reconstructed in this study. The model sets a fixed fuel burn time of 3ms and does not take into account the intake pressure and fuel injection volumes. Through the simulation optimization technology, the injection time at different speeds is systematically studied, aiming to find the fuel injection time that can make the engine performance the best at the optimal speed, and the simulation optimization details are shown in Figure 10.

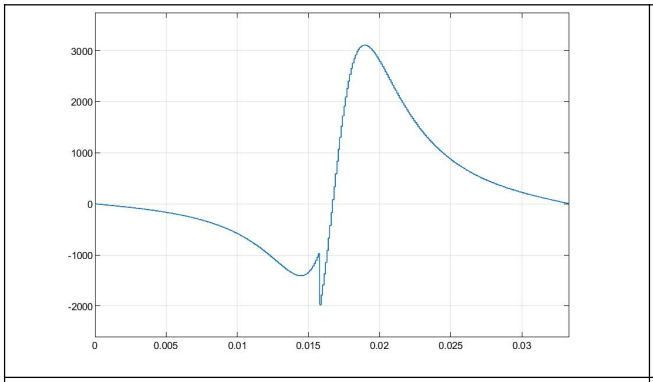

Fig8 The torque in previous model

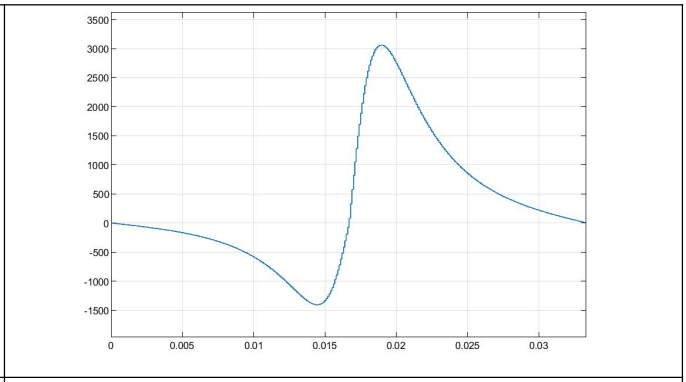

Fig9 The torque after adding the delay combustion

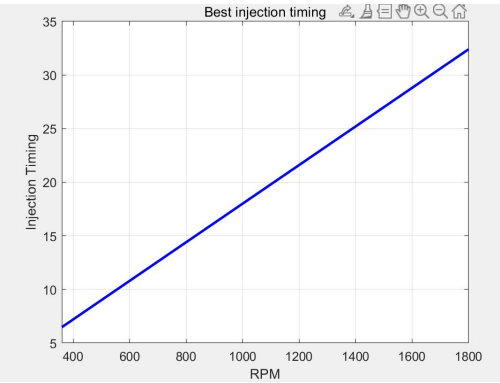

Fig10 Injection time for optimal thermal efficiency

2 Injection temperature and injection timing for optimal thermal efficiency

The objective of this study is to identify the optimal combination of Start of Injection and intake temperature that maximizes thermal efficiency while meeting a specified torque demand. The equivalence ratio (Φ) fixed at 0.8 to represent a typical lean mixture condition. The investigation is conducted at engine speeds from 360 to 1800—to explore how the optimal parameters vary with speed. An automated MATLAB-Simulink-based parameter sweep and optimization method is employed. For each fixed RPM, the torque target is set from 45 to 450 N · m. The script scans a two-dimensional parameter space defined by SOI and T_in. For each parameter pair, the fuel injection quantity is adjusted to maintain a constant equivalence ratio, then a Simulink simulation is executed to calculate the resulting torque and thermal efficiency. The results are visualized as two-dimensional MAPs where thermal efficiency is shown by background color and torque by contour lines. By highlighting the contour corresponding to the target torque and locating the point on this line with the highest thermal efficiency, the optimal control parameters can be determined.

By analyzing the simulation results and the corresponding maps (Fig12 13 14), we can draw two major conclusions regarding the optimal intake temperature and injection timing. Across all three tested engine speeds, the intake temperature that yields the highest thermal efficiency consistently falls at the lowest boundary of the search range, namely 350 K. This outcome aligns well with the predictions of ideal thermodynamic models. Under the constraint of a fixed equivalence ratio (Φ = 0.8), a lower intake temperature increases the air density, thereby requiring a greater amount of fuel to maintain the same Φ. As a result, the total heat released during combustion increases, producing a higher net work output and torque. Although the ideal Otto cycle assumes thermal efficiency to be independent of intake temperature, in the simulated scenario — where intake temperature affects charge mass and, consequently, fuel quantity and heat release—the point with the lowest intake temperature offers the highest energy utilization relative to compression losses. Therefore, it manifests as the global optimum in our simulation.

In terms of injection timing, a clear trend is observed as engine speed increases. At 600 RPM, the optimal start of injection is approximately 10.8 degrees before top dead center (BTDC). This value increases to about 14.4 degrees at 800 RPM and further to roughly 18.0 degrees at 1000 RPM. This progression is consistent with real engine behavior, where higher rotational speeds reduce the physical time available for the combustion process. To ensure that the combustion-induced pressure peak acts effectively on the piston shortly after TDC, it is necessary to advance the injection timing. This allows adequate time for fuel atomization, ignition delay, and complete combustion.

Tab3 Optimal parameter combination for 450 N · m torque (100%) output

RPM	Torque (100%)	SOI (deg) BTDC	Inlet Temperature (K)	Thermal Efficiency (%)
600	450	10.8	380	59.8
800	450	14.4	377	60
1000	450	18	376	60

Tab4 Optimal parameter combination for 405 N · m torque (90%) output

RPM	Torque (90%)	SOI (deg) BTDC	Inlet Temperature (K)	Thermal Efficiency (%)
600	405	10.8	420	59.8
800	405	14.4	419	59.9
1000	405	18	419	60

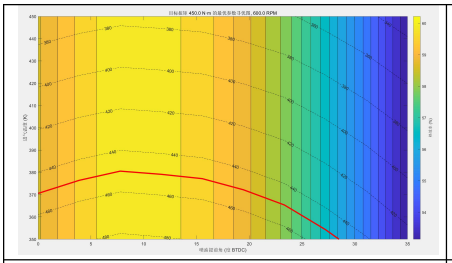

Fig11 Optimization results at 600 RPM

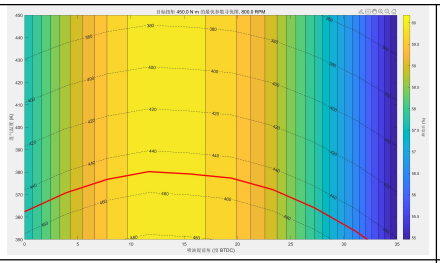

Fig12 Optimization results at 800 RPM

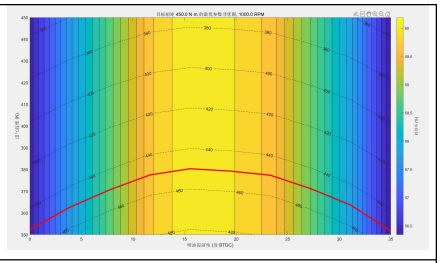

Fig13 Optimization results at 1000 RPM

V. *PID model system construction*

To simulate a typical driving acceleration scenario, this study defines the engine to accelerate smoothly from a low-load condition to a full-load state. The initial state corresponds to 20% of the rated speed (360 rpm) and 10% of the rated torque (40 N·m), while the target state is set at 100% of the rated speed (1800 rpm) and 100% of the rated torque (450 N·m). To ensure a dynamic yet smooth transition, a linear ramp function is employed to generate the target signals for the control system, with the entire acceleration process completed within 10 seconds. This setup represents a typical “full-throttle” acceleration condition, providing a representative test case for validating and optimizing the closed-loop control system.

The control system adopts a typical dual-loop cascade control strategy, consisting of an outer-loop speed controller and an inner-loop torque controller, enabling efficient closed-loop control over the engine’s acceleration process.

- The outer-loop controller takes the error between the target speed and the actual speed as input and outputs a desired torque signal, which serves as the control target for the inner loop.
- The inner-loop controller receives the desired torque and adjusts the fuel injection quantity to drive the engine output toward the desired value.
- The injection timing and intake pressure are treated as auxiliary control variables, obtained through interpolation using two-dimensional lookup tables (2-D Lookup Tables) based on the current engine speed and desired torque.

The complete structure of the control system is illustrated in the following figure.

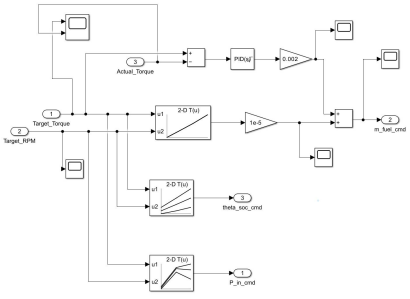

Fig.14 ECU PID controll system

1 Fuel Injection Calibration: Construction of a Speed–Torque 2D Lookup Table

This table is designed to provide a reference for fuel injection quantity estimation in engine control strategies. Specifically, it determines the required fuel injection amount under a given target engine speed (RPM) and torque condition.

Methodologically, for each fixed engine speed condition, the system iterates over a range of candidate fuel injection values. The engine model then calculates the resulting output torque for each case, and compares it to the target torque. The final selected injection value is the one that satisfies or most closely matches the target torque requirement.

This approach enables the construction of a three-dimensional lookup table mapping torque, engine speed, and fuel injection quantity. Such a table serves as a foundational element for real-time control, allowing the retrieval of optimal fuel commands under given operating conditions. Additionally, it provides essential input data for subsequent thermal efficiency analyses and multi-objective optimization tasks, such as minimizing fuel consumption and reducing emissions.

Table.5 Fuel Injection Quantity (1e-5g/cycle) at certain RPM and torque

Torque \ RPM	360	1000	1800
40	2.30	2.40	2.50
150	7.93	8.05	8.15
300	16.11	16.22	16.33
450	24.7	24.80	24.90

2 Injection Timing Calibration: Construction of a Speed–Torque 2D Lookup Table

The injection timing settings adopted at this stage are based on preliminary estimations derived from engine speed variations. The primary objective is to provide a feasible timing framework for establishing a closed-loop control system. This table does not further consider the coupled effects of fuel injection quantity and intake pressure on the combustion process.

Table.6 Injection Timing (deg) at certain RPM and torque

Torque \ RPM	360	1000	1800
40	6.48	18	25
150	6.48	18	25
300	6.48	18	25
450	6.48	18	25

3 Pressure Inlet Calibration: Construction of a Speed–Torque 2D Lookup Table

To investigate the impact of intake pressure on engine performance, a two-dimensional characteristic map was established, with engine speed and torque as inputs and intake manifold pressure as the output. In real-world operation, the dynamic response of intake pressure exhibits significant lag—particularly in turbocharged engines—a phenomenon commonly referred to as turbo lag.

This lag arises from physical inertia and the delay in pressurizing the intake plumbing, resulting in a measurable time delay between the control command and the actual rise in intake pressure. To approximate this delay behavior in the model, a Transport Delay module was introduced, with a delay time set to 10 ms.

Based on this, in order to achieve optimized fuel injection control—i.e., minimizing fuel injection quantity while maximizing thermal efficiency under given speed and torque demands—a two-dimensional thermal efficiency distribution map was constructed, using Start of Injection (SOI) and fuel mass as the coordinate axes. The visualization is presented as follows:

- Thermal efficiency is represented by color intensity, where brighter colors indicate higher efficiency.
- Torque levels are superimposed using contour lines, enabling the identification of solution spaces under specific load conditions.

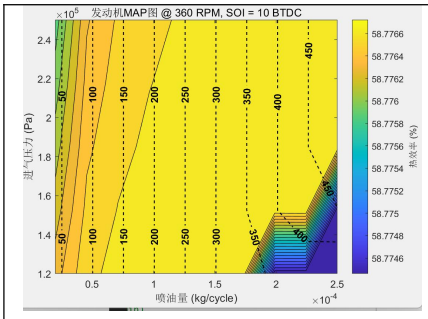

Fig15 2D Contour Plot of Engine Performance as a Function of Fuel Injection Quantity and Intake Pressure (360 RPM)

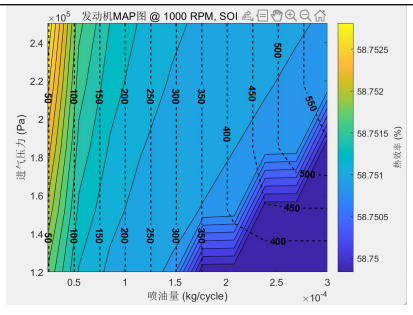

Fig16 2D Contour Plot of Engine Performance as a Function of Fuel Injection Quantity and Intake Pressure (1000 RPM)

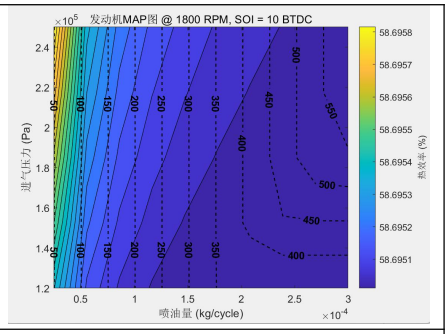

Fig17 2D Contour Plot of Engine Performance as a Function of Fuel Injection Quantity and Intake Pressure (1200 RPM)

Table.7 Pressure inlet (Pa) at certain RPM and torque

Torque \ RPM	360	1000	1800
40	1.2	2.3	2.3
150	1.2	2.3	2.3
300	1.2	2.3	2.3
450	1.7	1.8	2.4

4 PID model evaluation

To evaluate the performance of the designed PID controller, a simulation was conducted using a linearly ramping target torque signal. As shown in the figure, the system's output torque (blue curve) closely follows the target torque trajectory (yellow curve), demonstrating excellent dynamic tracking behavior. Specifically, the controller achieves near-zero steady-state error, fast response time, and negligible overshoot or oscillation throughout the entire operation, reflecting strong performance in terms of accuracy, responsiveness, and stability.

In addition, the step-like appearance of the output torque is consistent with the adopted control strategy, which updates the average torque feedback once per engine cycle. This confirms the validity of the closed-loop logic. Notably, as engine speed increases, the feedback update interval shortens, leading to narrower steps, which indicates that the controller's response frequency scales appropriately with engine operating conditions. In

summary, the PID controller has been tuned to a near-optimal state under the tested conditions and demonstrates strong practical applicability.

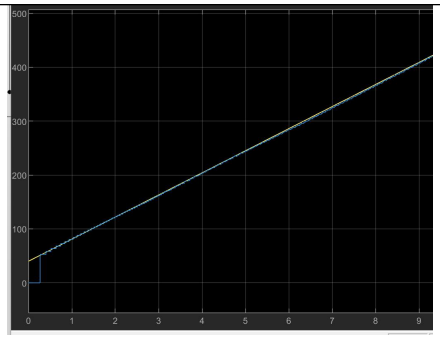

Fig18 PID Torque tracking diagram

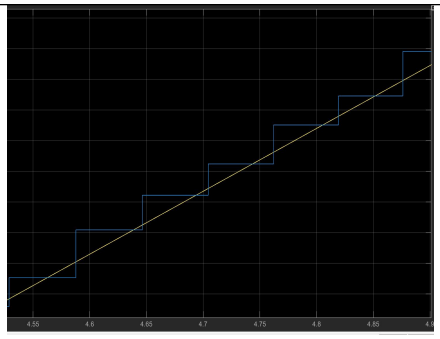

Fig18 PID Torque tracking diagram zoom in

VI. Control Strategy Optimization: Design and Verification of PID Controller Based on Segmented Gain Scheduling

In the dynamic control simulation of the engine acceleration process, the basic PID controller adopts a fixed set of gain parameters (Kp, Ki, Kd), although it can provide a good response in the low-speed and low-load stage, but after entering the high-speed and high-load range, due to the significant changes in the dynamic characteristics of the engine, the control system gradually exposes the problems of increased tracking error and response lag. The essential reason for this deterioration is that the nonlinear response of the engine varies significantly over different operating intervals, and the fixed-parameter PID controller cannot adapt to this condition-dependent variation.

In order to solve the above problems, this study proposes a control strategy based on Piecewise Gain Scheduling. In this method, the whole acceleration process is divided into two stages: $t < 5$ s for the low-speed/low-load section, and $t \geqslant 5$ s for the high-speed/high-load section. Within each stage, a set of individually optimized PID parameters is selected to better match the dynamic response characteristics of the engine at that stage. This method is equivalent to introducing the idea of "local optimum" into the controller, which improves the flexibility and accuracy of the control strategy. Parameter switching is done via the Switch module in Simulink, controlled by a Clock signal, which automatically switches the gain when the simulation time reaches 5 seconds.

The simulation results show that compared with the fixed-gain PID controller, the segmented gain controller exhibits better tracking accuracy and stronger dynamic

adaptability during the whole acceleration process. Especially in the second half of acceleration, the original controller began to have obvious lag and steady-state error, while the optimized controller can continue to adhere to the target torque curve, effectively making up for the response defects of the original system. Furthermore, the integrated absolute error (IAE) index is quantitatively evaluated, and the segmented control strategy significantly reduces the error from the original 50 to 25, which verifies the significant effect of the method in improving the control quality.

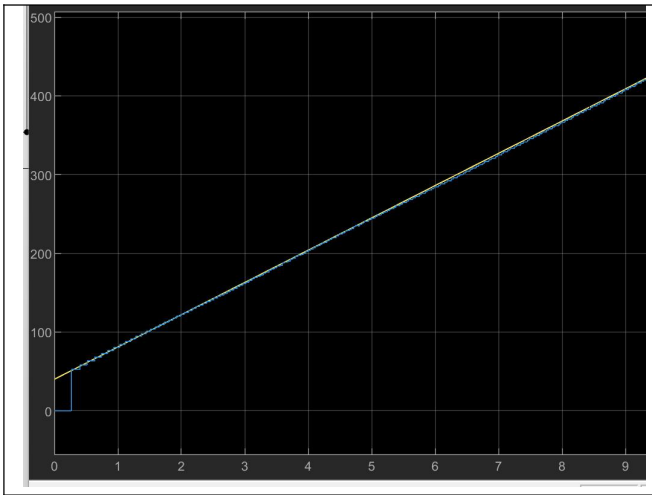

Fig20 Previous PID Controller System

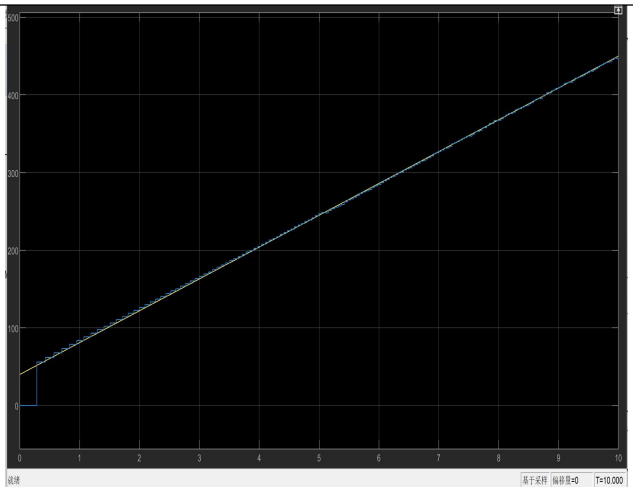

Fig21 PID Controller Based on Segmented Gain Scheduling

References

[1] Dorf, R. C. (2014). The Electrical Engineering Handbook. CRC Press.

[2] Ziegler, J.G., & Nichols, N.B. (1942). Optimum Settings for Automatic Controllers. Journal of Fluids Engineering.

[3] Li, S., & Lv, F. (2012). Feedforward compensation based the study of PID controller. Advances in Electronic Commerce, Web Application and Communication: Volume 2, 59-64.